CHIMIA **2002**, *56*, No. 11

Chimia 56 (2002) 647–653

ISSN 0009–4293

Application of Microstructured Reactor Technology for the Photochemical Chlorination of Alkylaromatics

Heike Ehrich[a], David Linke[a], Konrad Morgenschweis[b], Manfred Baerns[a], and Klaus Jähnisch[a]*

Abstract: The advantageous application of a falling-film microreactor for a photochemical gas/liquid reaction was demonstrated by the selective photochlorination of toluene-2,4-diisocyanate (TDI). In the microstructured reactor the selectivity to the side-chain chlorinated product 1-chloromethyl-2,4-diisocyanatobenzene (1Cl-TDI) achieved a value of 80% at 55% TDI conversion, whereas the side product toluene-5-chloro-2,4-diisocyanate (5Cl-TDI) was formed with only 5% selectivity. The yield of 1Cl-TDI was enhanced by increasing the residence time from 24% after 5 s to 54% after 14 s. At the same time the formation of consecutive products increased and the selectivity to 1Cl-TDI decreased to 67% after 14 s residence time. The influence of the reactor material was shown. In presence of a Lewis acid such as $FeCl_3$, formed by chlorination using a reaction plate made of iron, consecutive products were formed and the selectivity to 1Cl-TDI was lowered. The microstructured reactor led to remarkably higher selectivities than the conventional batch reactor, where the selectivity to 1Cl-TDI was only 45% at 65% TDI conversion and the side product 5Cl-TDI was formed with 50% selectivity. The space-time yield of 1Cl-TDI achieved in the microstructured reactor (400 mol l^{-1} h^{-1}) clearly exceeded the performance of the batch reactor (space-time yield 1.3 mol l^{-1} h^{-1}). Based on the microreactor data, a kinetic model for the TDI chlorination including by-product formation was suggested and used to predict product selectivity at full TDI conversion.

Keywords: Gas/liquid reaction · Microstructured reactor · Photochlorination

1. Introduction

In recent years microstructured reactors have attracted increasing interest as useful devices for chemical reactions and processes. Basic features of such reactors are their high surface area to internal volume ratio, resulting from channel widths of less than 1000 μm. This leads to a much better heat removal for exothermic reactions than in macroscopic batch reactors. Accumulated reaction heat leading to hot spots, which are responsible for parallel, consecutive and decomposition reactions, is suppressed. As a result, higher selectivities, yields and product qualities are usually obtained. Moreover, the reactions proceeding in a small volume can be controlled much more easily with respect to pressure, temperature, and residence time. Thus, the risk of highly exothermic or explosive reactions can be reduced drastically.

An overview on the application of microstructured reactors to fine chemical synthesis has been given by de Mello and Wootton [1]. Clear advantages are shown in comparison to existing technologies in direct fluorination [2], nitration of organic compounds [3], catalytic gas-phase reactions [4][5], exothermic gaseous reactions [6], diazotization of aromatic amines [7] and photochemical reactions [8][9], because in microstructured devices a rapid heat and mass transfer is enabled due to small diffusion distances within the microchannels. Only few examples for the application of microstructured reactors for gas/liquid reactions have been reported. Recently, it could be shown that the direct fluorination of toluene with elemental fluorine gives noticeably higher selectivities and space-time yields when conducted in a falling-film microreactor or a micro bubble column compared to a laboratory bubble column [2].

Photochemical methods using light as an ecologically clean 'reagent' offer more selective routes for chemical processes than thermal ones. Nevertheless, photochemical and thermal methods are often complementary techniques leading to safer and less time-consuming syntheses [10]. However, the disadvantage of poor spatial illumination homogeneity in photochemical reactions has to be compensated by the reactor design. Industrial photochemical processes are auspiciously performed in large tubular reactors directly irradiated from the outside by macro-scale lamps [11]. This type of reactor allows a broad variety of reactions. However, in large-scale photochemical re-

*Correspondence: Dr. K. Jähnisch
Tel.: +49 30 6392 4146
Fax: +49 30 6392 4350
E-Mail: jaehnisch@aca-berlin.de
[a]Institut für Angewandte Chemie Berlin-Adlershof
Richard-Willstätter-Str. 12
D-12489 Berlin, Germany
[b]BASF Schwarzheide GmbH
Schipkauer Str. 1
D-01986 Schwarzheide, Germany

actors the light penetrates only a small reaction zone near the wall of the reactor and large amounts of the substrate are not irradiated. This disadvantage arises from the dependence of absorbance of a radiation beam from the absorption path length according to the Lambert-Beer law. To overcome this disadvantage photochemical reactions are often performed in falling-film reactors, where the surface of a thin film containing the liquid substrate is irradiated [11]. Using miniaturized reaction systems the film is less than 100 μm thick and the light penetrates through most of the depth of the fluid.

The advantageous application of microstructured reactors for photochemical reactions has been demonstrated by Jensen and coworkers [8] in 2001 and de Mello and coworkers [9] in 2002. Jensen *et al.* showed the high efficiency of photon transfer using micro-fabricated chip devices as reactors. The pinacol formation from benzophenone, which follows a free-radical mechanism, was studied as a model reaction. Known scale-up difficulties in photochemical reactions due to poor illumination uniformity and excessive sample heating have been overcome by parallel operations of multiple miniaturized reaction devices [8]. De Mello used a nano-scale reactor for the protected and continuous generation and reaction of singlet oxygen without the inherent danger of large quantities of oxygenated solvents. The introduction of a peroxy function by cycloaddition of singlet oxygen was demonstrated by the photooxidation of α-terpinene to ascaridole [9]. The authors have shown that the microreactor technique allows effective irradiation even with low intensity light sources.

In the future, microstructured reactors will play an increasing role in chemical industry. With this paper we contribute to the for industrial important processes. The performance of microstructured reactors is demonstrated by the photochlorination of the side chain in alkylaromatics. The gas/liquid reaction of toluene-2,4-diisocyanate (TDI) with chlorine to form 1-chloromethyl-2,4-diisocyanatobenzene (1Cl-TDI), being an intermediate for the synthesis of polyurethanes, is used as an exemplary reaction. Toluene-5 chloro-2,4-diisocyanate (5Cl-TDI) is a side product of the chlorination. Data used for selectivity and conversion were taken depending on residence time and on the material (Ni or Fe) chosen for the microstructured reactor. The results were furthermore compared with those obtained in a batch reactor.

2. Photochlorination of Toluene-2,4-diisocyanate

Chlorination of alkylaromatic compounds by substitution of hydrogen by a halogen atom is a typical example of a free-radical chain reaction. Reaction (1), see Scheme 1, is started by the generation of chlorine free radicals by irradiation (reaction (3)). 1-Chloromethyl-2,4-diisocyanatobenzene (1Cl-TDI) is formed by side-chain chlorination of TDI (reactions (4) and (5)) following a free-radical mechanism.

However, high local concentration of

$$Cl_2 \xrightarrow{h\nu} (Cl_2)^{\cdot} \longrightarrow 2\,Cl^{\cdot} \quad (3)$$

$$Ar\text{-}CH_3 + Cl^{\cdot} \longrightarrow Ar\text{-}CH_2^{\cdot} + HCl \quad (4)$$

$$Ar\text{-}CH_2^{\cdot} + Cl_2 \longrightarrow Ar\text{-}CH_2Cl + Cl^{\cdot} \quad (5)$$

newly formed chain-starting radicals favors their recombination or undesired secondary reactions and reduces the chain chlorination. Thus, the economy of photochlorination decreases.

Beside the side-chain chlorinated product 1Cl-TDI, the ring-chlorinated product 5Cl-TDI is formed in a parallel reaction (reaction (2) in Scheme 1), and products of hydrolysis or polycondensation can be formed as consecutive products. The formation of the side product 5Cl-TDI by electrophilic substitution can be suppressed by carrying out the reaction at elevated temperatures and irradiation. But electrophilic substitution is catalyzed by Lewis acids acting as halogen transmitter, which are formed by chlorination of metallic impurities, *e.g.* Fe^{3+} [12]. Benzylchlorides such as the target product 1Cl-TDI also react with Friedel-Crafts catalysts like $FeCl_3$ by separation of halogen chloride to give resin-like condensation products [13]. For this reason, the influence of iron was investigated by carrying out the reaction in microstructured devices made of nickel and iron, respectively.

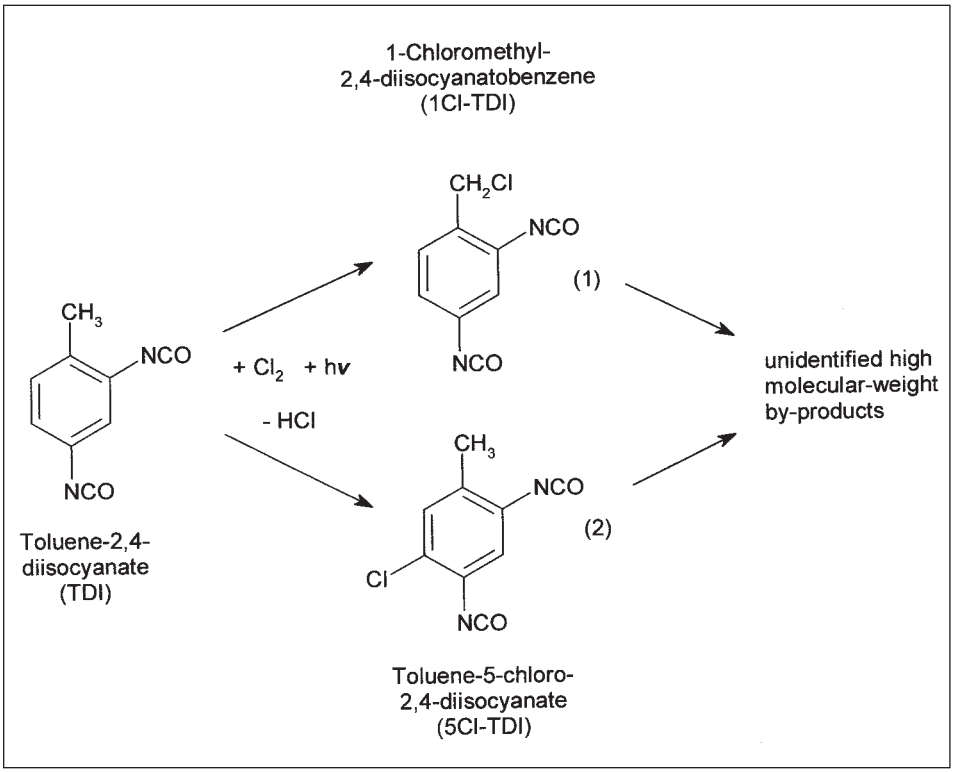

Scheme 1. Photochlorination of toluene-2,4-diisocyanate (TDI) forming 1-chloromethyl-2,4-diisocyanatobenzene (1Cl-TDI), depicted in reaction (1), and toluene-5-chloro-2,4-diisocyanate (5Cl-TDI) as a side-product in reaction (2).

3. Experimental

3.1. *Microreactor Design and Equipment*

A falling-film microreactor, which generated thin films by contacting liquid and gaseous phases, was applied. The reactor, designed by the Institut für Mikrotechnik Mainz, Germany, see [2], consists of a vertically orientated reaction plate containing 32 parallel microchannels (see Fig. 1). The channel width is 600 μm, the depth 300 μm and the length is 66 mm. Two plates were

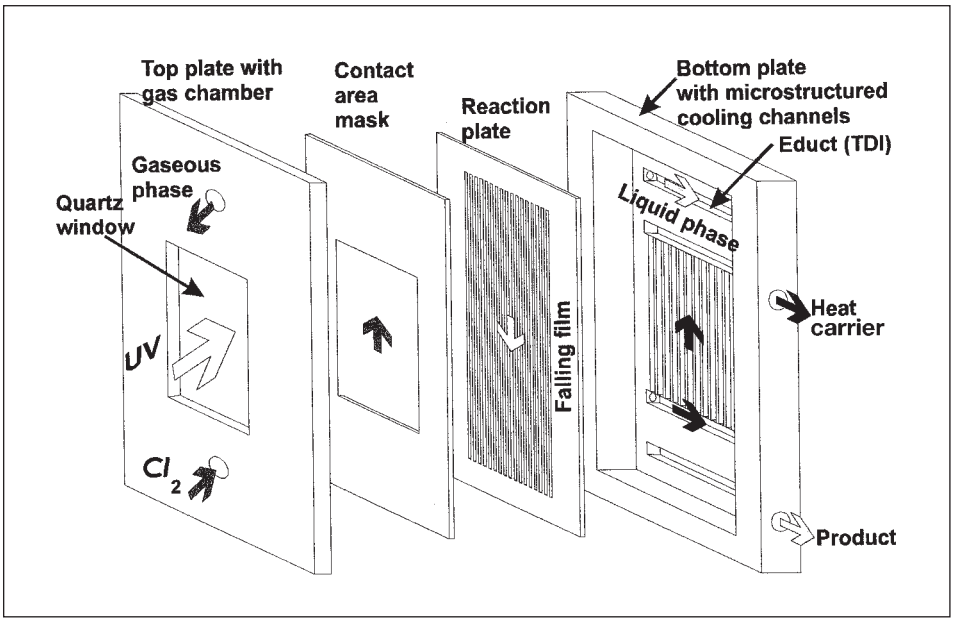

Fig. 1. The microstructured reactor device (source: Institut für Mikrotechnik Mainz, IMM) with inlets and outlets for the gas, the liquid phase, and the heat carrier.

used: reactor module 1 was made of nickel, and reactor module 2 of iron.

In the falling-film configuration, the liquid phase is introduced into the microreactor device by a horizontal slot (see Fig. 1). The solution is then distributed to substreams, which enters a microchannel through an orifice and flows downwards. A thin film of the liquid reactant is generated by gravity force. The gaseous phase was passed counter currently to the liquid phase through the microreactor device, and the chemical reaction took place at the interface between liquid and gaseous component. The thickness of the fluid in the falling-film reactor was calculated based on film theory according to Eqn. (6) given by Perry [14], where δ = film thickness, $\dot{V}_{liq}$ = liquid flow rate, η_{liq} = viscosity of the liquid, ρ_{liq} = density of the liquid, B = width of the film, and g = acceleration due to gravity. Depending on the volumetric flow the film thickness was calculated to be 21 µm to 36 µm, see Table 1.

This calculation allows an approximation of the real film thickness for laminar flow of low-viscosity liquids. However, the applicability of this method for microstructured devices with the large surface to volume ratio is unknown. First attempts to measure the film thickness in microreactors were made by Wille [15]. The results showed a significant deviation between the calculated data and the measured film thickness of about 50%, which were explained by the influence of wall effects.

$$\delta = \left[\frac{3\ \dot{V}_{liq}\ \eta_{liq}}{\rho_{liq}\ B\ g} \right]^{1/3} \qquad (6)$$

For photochemical reactions the microreactor was equipped with a transparent quartz window (see Fig. 1) for light penetration into the channels of the reactor. The reactants were irradiated using an unfiltered 1000 W Xenon lamp (LAX 1000, Müller Elektronik-Optik, Moosinning, Germany) located in front of the window. The wavelength was in the range of 190 nm to 2500 nm with maximum intensity at about 800 nm.

3.2. *Chemical Reaction*

A solution of TDI (100 mmol = 14.4 ml) in tetrachloroethane (30 ml) was prepared. The solution was introduced into the reactor at flow rates of 0.12 ml/min, 0.23 ml/min, 0.38 ml/min, and 0.57 ml/min. The flow was controlled by a pump with PTFE pump head (Masterflex®). Variation of liquid flow rates changed residence times, too, achieving 13.7 s at 0.12 ml/min, 8.9 s at 0.23 ml/min, 6.6 s at 0.38 ml/min, and 4.8 s at 0.57 ml/min, see Table 1. The gas-flow rates of chlorine were between 14 ml/min and 56 ml/min (measured by a mass-flow controller, Bronckhorst) to ensure equimolar ratio of TDI to chlorine.

The backside of the reaction plate was held at the desired reaction temperature of 130 °C by a continuously flowing heat carrier. Temperatures were controlled by thermocouples at the inlet and the product outlet. The product was continuously removed from the reactor by a pump. Inlets and outlets of the reactor were connected with the liquid and gaseous components by PTFE tubing with standard fittings.

3.3. *Reactions in a Batch Reactor*

Batch reactions were carried out in a flask, where the lamp is located in a tube pipe surrounded by the reaction solution. A mercury high-pressure lamp was used as irradiation source. The vessel containing 100 mmol of TDI in 30 ml tetrachloroethane was heated by an oil bath to 130 °C and continuously stirred. Chlorine was bubbled through the solution during continuous irradiation. The molar ratio of TDI to Cl was varied ranging from 1:2, 1:1, to 2:1. The reaction was interrupted after 30 min of chlorination.

3.4. *Analysis*

The product stream of the continuously operated reactor was collected in a glass vessel. For analysis samples were taken directly from the microstructured reactor outlet after 30 min, 40 min and 60 min of continuous flow under irradiation, each with two samples. 100 µl of the product were diluted in a ratio of 1:10 with toluene containing 1,4-dichlorobenzene as internal standard and analyzed by GC using a

Table 1. Film thickness, liquid reaction volume, specific interfacial area, and residence time by variation of volumetric flow rate calculated for the microstructured reactor device based on film theory [14].

Flow rate [ml TDI/min]	Film thickness[a] [µm]	Film volume[b] [ml]	Interfacial area [m^2/m^3]	Residence time [s]
0.12	21	0.027	48000	13.7
0.23	27	0.034	37000	8.9
0.38	33	0.042	30000	6.6
0.57	36	0.046	28000	4.8

[a] referred to a channel width of 600 µm and a channel number of 32
[b] microreactor with 32 microchannels á 600 µm × 300 µm × 64 mm

SUPELCO SPB-50 column (length 30 m, ID 0.25 mm), FID as detector, and helium as carrier gas.

For each experiment, conversion X of TDI, yield Y of 1Cl-TDI and selectivity S to 1Cl-TDI based on conversion of TDI, as well as selectivity to the side product 5Cl-TDI were determined. An average was generated from six values obtained for each experiment. The standard deviations of conversion and selectivity amounted to about 5%. The performance of the reactors was characterized by the space-time yield of 1Cl-TDI. The reaction volume was calculated as film volume inside of the microchannels. Thus, the internal volume of the microreactor device was omitted and only a fluid film of 21 to 36 µm thickness was taken into account and not the total channel depth of 300 µm. At a volumetric flow rate of 0.57 ml/min the film volume amounted to 0.046 ml, considering the number and width of the microchannels, see Table 1. The specific interfacial area of the falling film, see Table 1, was calculated as reciprocal value of the film thickness, *e.g.* the ratio of film surface to the liquid reaction volume.

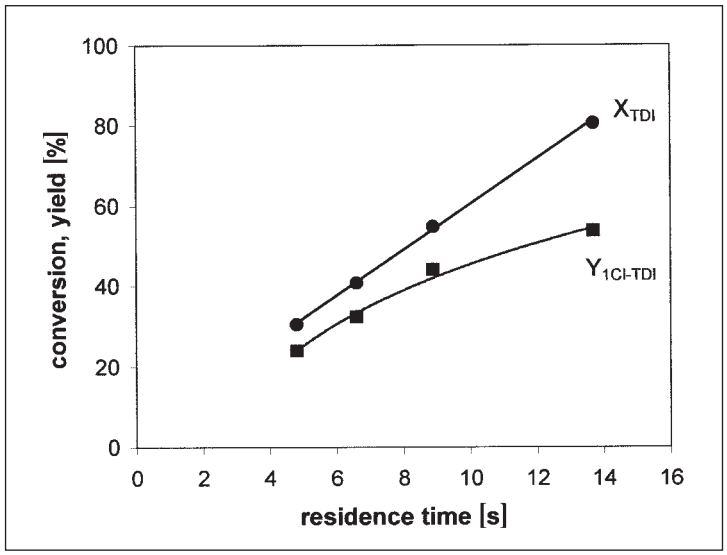

Fig. 2. Photochlorination of TDI: Effect of residence time on TDI conversion and yield of 1Cl-TDI for the reaction using microreactor module 1 (nickel plate). Reaction conditions: molar ratio TDI:Cl = 1:1, temperature 130 °C.

4. Results and Discussion

4.1. *Variation of Residence Time*

Efficient contacting between liquid and gaseous phase is a primary task of microstructured reactors and is considerably influenced by the residence time of the reactants inside the channels. Residence time was varied by changing the flow rate of TDI ranging from 0.12 ml/min to 0.57 ml/min.

Increasing residence time results in smaller film thickness, see Table 1, and mass transport between gaseous and liquid phase is enhanced. This is expressed by the rising specific interfacial area, and the transport of chlorine or chlorine radicals into the liquid film is advantaged. Consequently, conversion of toluene-2,4-diisocyanate increased from 30% to 81%, while the selectivity to the target product 1Cl-TDI decreased from 80% to 67%. The results of TDI conversion and selectivities using the microstructured reactor module 1 (nickel plate) are given in Table 2.

Conversion of TDI as well as yield of 1Cl-TDI are depicted in Fig. 2 as a function of residence time. The more efficient mass exchange between gaseous and liquid phase at larger residence times resulted in a higher TDI conversion. The product yield increased from 24% after 5 s (TDI flow rate 0.57 ml/min) to 54% after 14 s residence time (TDI flow rate 0.12 ml/min). However, at longer residence time than about 14 s the yield of 1Cl-TDI probably will no longer increase significantly.

The performance of the reactor module 1 is shown in a selectivity-conversion diagram in Fig. 3, where selectivity to 1Cl-TDI, to the side product 5Cl-TDI as well as to further by-products are depicted depending on TDI conversion. Selectivity to the side-chain chlorinated product 1Cl-TDI amounted to 80% and remained unaffected by TDI conversion ranging from 30% to 55%. At higher TDI conversion, obtained at longer residence time, 1Cl-TDI selectivity decreased to 67%. On the other hand, selectivity to the ring-chlorinated side product 5Cl-TDI decreased with enhanced TDI conversion from 12% at 30% conversion to 5% at 80% conversion. The difference between TDI conversion and the sum of products observed by GC is expressed in Fig. 3 as graph for by-products. The increased selectivity to the by-products at higher TDI conversion gave evidence that by-products are mostly formed by consecutive reactions, to which the decreased selectivity to 1Cl-TDI and to 5Cl-TDI can be attributed. We can conclude that in microstructured reactors a high performance was obtained when short residence times were chosen and thus, consecutive reactions were avoided.

Table 2. TDI conversion, selectivities and space-time yield of 1Cl-TDI using reactor module 1[a] (nickel plate) for various flow rates.

Flow rate [ml TDI/min]	X [%]	$S_{1Cl\text{-}TDI}$ [%]	$S_{5Cl\text{-}TDI}$ [%]	STY[b] [mol l^{-1} h^{-1}]
0.12	81	67	5	321
0.23	55	80	5	401
0.38	41	79	8	393
0.57	30	79	12	398

[a] 32 microchannels á 600 µm × 300 µm × 64 mm
[b] referred to the film volume in the microchannels

4.2. *Variation of the Material of the Reaction Plate*

Lewis acids are known as catalysts for the chlorination of the aromatic ring; they act as a chlorine transmitter. Furthermore, the chloromethyl group in 1Cl-TDI can react with Lewis acids forming condensation products by separation of HCl. If the reactor device contains *e.g.* iron, Lewis acids like Fe(III) chloride are formed by chlorination. To investigate the influence of Fe the reaction was additionally performed in a reactor containing an iron plate (reactor module 2).

Conversion and selectivities obtained for the reaction are shown in Table 3 at different flow rates. Comparing the results with those obtained in reactor module 1 (Table 2) it can be concluded that the se-

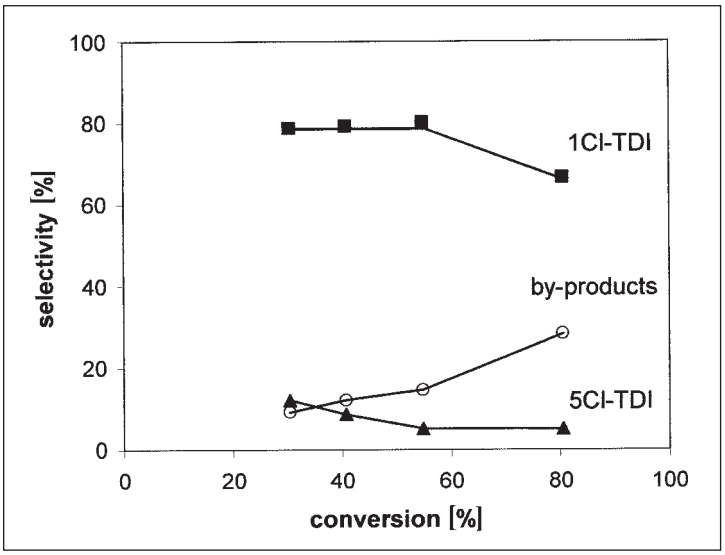

Fig. 3. Photochlorination of TDI: Selectivities of main and side product as a function of TDI conversion for the reaction using microreactor module 1 (nickel plate). Reaction conditions: molar ratio TDI:Cl = 1:1, temperature 130 °C.

Table 3: TDI conversion, selectivities and space-time yield of 1Cl-TDI using reactor module 2[a] (iron plate) for various flow rates.

Flow rate [ml TDI/min]	X [%]	$S_{1Cl\text{-}TDI}$ [%]	$S_{5Cl\text{-}TDI}$ [%]	STY[b] [mol l^{-1} h^{-1}]
0.12	80	50	5	236
0.24	56	65	4	346
0.35	43	59	5	288
0.57	31	64	10	333

[a] 32 microchannels á 600 µm × 300 µm × 64 mm
[b] referred to the film volume in the microchannels

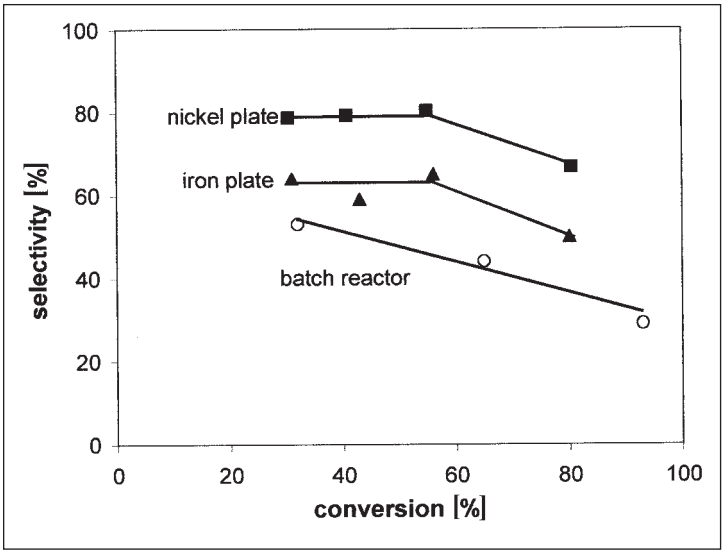

Fig. 4. Selectivity for 1Cl-TDI depending on TDI conversion compared for the reaction in the microstructured reactor module 1[a] (nickel), module 2[a] (iron) and in the batch reactor[b]. Conditions: a) molar ratio of TDI:Cl was 1:1, b) molar ratio of TDI:Cl was 2:1, 1:1, and 1:2, reaction temperature 130 °C.

lectivity to the target product 1Cl-TDI (side-chain chlorination) was strongly affected by the plate material, whereas the selectivity to the side product 5Cl-TDI was not significantly influenced. At 80% TDI conversion, using the iron plate selectivity to 1Cl-TDI amounted to 50%, whereas using the nickel plate 67% selectivity was achieved. The same trend was observed at smaller TDI conversion.

This result gives evidence on the enhanced formation of consecutive products from 1Cl-TDI in the presence of Lewis acids. These products, probably resin-like condensation products, could not be identified by GC, but solid particles were observed in the collecting tank. An enhanced formation of the ring-chlorinated side product 5Cl-TDI by using the iron reaction plate could not shown.

4.3. *The Advantage of a Microreactor in Photochlorination*

The photon efficiency is one of the most important criteria of a photochemical reaction. The radicals are generated by irradiation of chlorine (reaction (3) in section 2) and tend to recombine if their concentration is too high. As a consequence of that, recombination of the radicals can be suppressed by avoiding high local radical concentration in the whole reactor. This is facilitated by the high specific interfacial area in microreactor devices designed for carrying out gas/liquid reactions. Due to the fast mass transfer of chlorine into the liquid and the fast diffusion within the liquid film, chlorine is spread effectively over the liquid phase, where the reaction occurs. In contrast, in conventional reactors radical concentration near the reactor wall is high and small in the internal volume of the reactor.

The photochlorination of TDI in the microreactor was performed at short residence times, resulting in a space-time yield of 1Cl-TDI using module 1 of 401 mol l^{-1} h^{-1} at 55% TDI conversion, see Table 2. The selectivity to the target product 1Cl-TDI amounted to 80% and the ring-chlorinated product 5Cl-TDI was formed with only 5% selectivity. The space-time yield exceeded those of the batch reactor in orders of magnitude and the selectivity of 1Cl-TDI by a factor of two. Using the batch reactor space-time yield amounted to only 1.3 mol 1Cl-TDI l^{-1} h^{-1} at 65% TDI conversion during 30 min. The 1Cl-TDI selectivity was merely 45%, whereas the side product 5Cl-TDI was obtained with 54% selectivity.

The performance of the reactors is compared in Fig. 4, where selectivity of 1Cl-TDI obtained for the reaction in the microstructured reactor modules 1 (nickel plate) and 2 (iron plate) are compared to those ob-

tained with the batch reactor as a function of TDI conversion. The largest 1Cl-TDI selectivity was obtained using the microstructured reactor module 1. In contrast, using the batch reactor selectivity was significantly smaller, resulting from the formation of the ring-chlorinated side product. These results clearly demonstrate the improved performance of the microreactor.

The effect on selectivity is explained with a more efficient photon yield in the small volume of the microstructured reactor devices compared to ideal batch reactors. The photochemical induced chlorination of alkylaromatics leads to a high selectivity of the alkyl-chain chlorinated product, since the light can easily penetrate through a thin film of the substrate and chlorine radicals are present within the whole film depth. In contrast, in a reaction vessel light penetrates only in a small segment of the reactor. Most of the substrate is not induced by photon energy leading to side reactions. Without irradiation, the chlorination at the aromatic ring is favored resulting in the formation of 5Cl-TDI. In a conventional batch reactor photochlorination leads to a high local concentration of chlorine radicals and their recombination reduces the chlorination of the alkyl chain. The radicals cannot react quickly enough with the alkylaromatic species to produce the chlorinated product following in recombination of the radicals.

4.4. *Kinetics and Reaction Engineering*

In the present study gas-phase chlorine partial pressure was constant within the reactor since it was undiluted. Estimates showed that the diffusion transport of chlorine into the liquid layer is very fast as compared to the chemical reaction; from this it can be concluded that chlorine concentration either in molecular or atomic form is constant within the liquid phase. Under these conditions a kinetic model assuming a plug-flow reactor is reasonable.

According to Beltrame and Carra [16] the photochlorination of alkylated aromatic compounds is first order both in chlorine and in the organic substrate. Thus, the microreactor kinetic data, *i.e.* concentrations of TDI and of the two primary products (1Cl-TDI and 5Cl-TDI) were initially fitted to first order rate equations with respect to TDI, but we could not confirm this dependence. Finally, an order of 0.1 was calculated by simulation. In the final model, see Scheme 2, this value was approximated by a 0th order. The final model for the photochlorination includes the parallel reactions of TDI to 1Cl-TDI (P1) and to 5Cl-TDI (P2) being 0th order reactions with respect to TDI. Consecutive reaction steps as indicated in Scheme 2 forming product P3 (or some more products P4, P5 ..) were also considered. By fitting the model to the kinetic data it turned out that the consecutive reactions could be described best as 2nd order reactions. The estimated kinetic parameters are summarized in Scheme 2. These data were used to simulate the performance of a plug-flow type microstructured reactor, *i.e.* for determining the contact time required for reaching certain TDI and product concentration, see Fig. 5. The simulated data show good agreement

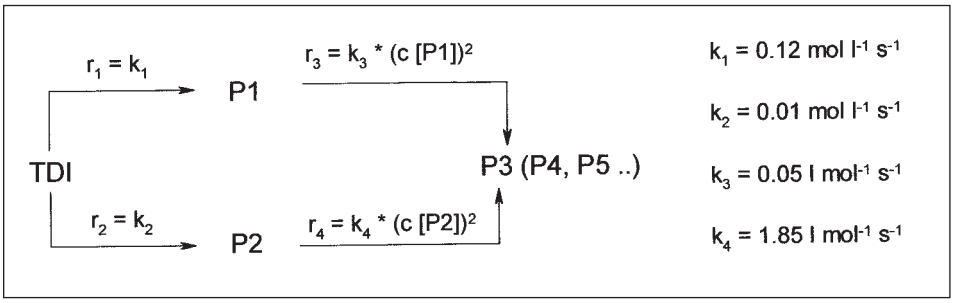

Scheme 2. Reaction network and rate equations of the final kinetic model, where P1 is the target product 1Cl-TDI, P2 the side product 5Cl-TDI, and P3 (P4, P5...) are high molecular consecutive products, and k_i are the respective rate constants.

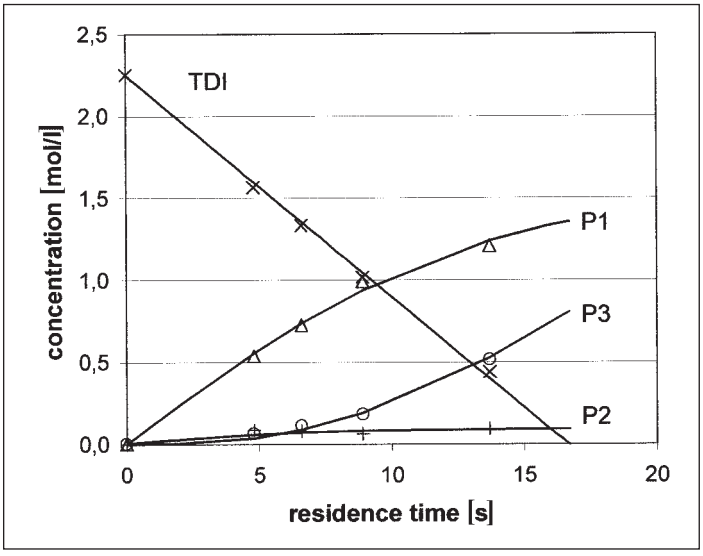

Fig. 5. Concentration of TDI and of the reaction products as a function of residence time - comparison between model (black lines) and experimental data obtained in the microreactor module 1 (points).

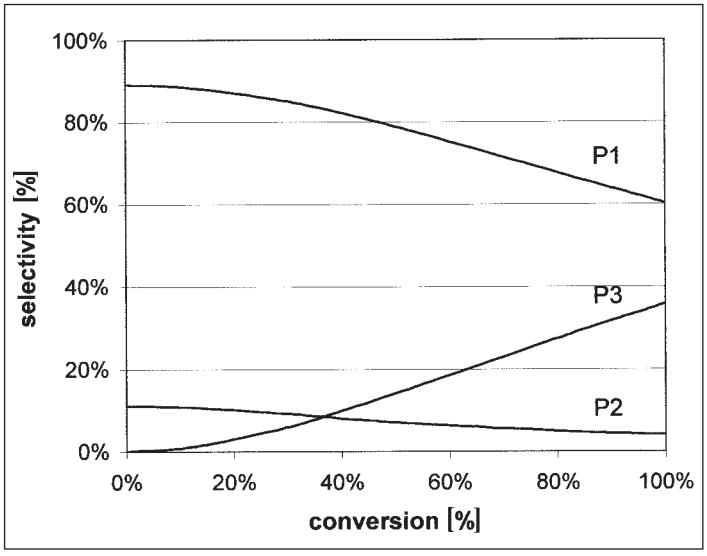

Fig. 6. Simulated selectivity versus TDI conversion curves based on the reaction network in Scheme 2.

with the experimental results. On this basis the required reactor size and the number of parallel reactors necessary for a given capacity can be calculated.

The plot of selectivity versus degree of TDI conversions (see Fig. 6) allows the selectivities to be estimated for a given TDI conversion and shows a severe loss in TDI selectivity when approaching full conversion. Thus, for industrial practice the reactor should presumably be operated at the maximal achievable yield of TDI.

5. Conclusions

The advantageous use of a microstructured reactor to perform a photo-induced gas/liquid reaction has been demonstrated by the photochlorination of toluene-2,4-diisocyanate. Compared to a batch set-up in miniaturized photochemical reactors light penetrates through most of the reactor depth. By the high surface to volume ratio in microstructured reactor devices the local concentration of chlorine radicals is significantly lower and clearly higher selectivities of the target product 1-chloromethyl-2,4-diisocyanatobenzene were achieved than using a conventional batch reactor. The space-time yield of the microstructured reactor was orders of magnitude higher compared to a conventionally reactor. Due to the advantageous mass transfer characteristics of the microreactor, intrinsic kinetic data were measured in the experiments, which facilitated the kinetic modeling of the TDI chlorination. A reaction network taking into account by-product formation has been suggested, which shows good agreement with the experimental data.

The present study describes a successful application of a falling-film microreactor for a photochemical gas/liquid reaction. It can be expected that the application of microreactors can also be beneficial to other photochemical reactions.

Received: October 14, 2002

[1] A. de Mello, R. Wootton, *Lab Chip* **2002**, *2*, 7.
[2] K. Jähnisch, M. Baerns, V. Hessel, W. Ehrfeld, V. Haferkamp, H. Löwe, C. Wille, A. Guber, *J. Fluorine Chem.* **2000**, *105*, 117.
[3] J.R. Burns, C. Ramshaw, *Proc. of the 4th International Conference on Microreaction Technology*, March 5–9 **2000**, Atlanta, p. 133.
[4] P. Claus, D. Hönicke, T. Zech, *Catal. Today* **2001**, *67*, 319.
[5] O. Wörz, K.P. Jäckel, T. Richter, A. Wolf, *Chem. Eng. Sci.* **2001**, *56*, 1029.
[6] E.V. Rebrov, M.H.J.M. de Croon, J.C. Schouten, *Catal. Today* **2001**, *69*, 183.
[7] H. Salimi-Moosavi, T. Tang, D.J. Harrison, *J. Am. Chem. Soc.* **1997**, *119*, 8716.
[8] H. Lu, M.A. Schmidt, K.F. Jensen, *Lab Chip* **2001**, *1*, 22.
[9] R.C.R. Wootton, R. Fortt, A.J. de Mello, *Org. Process Res. Dev.* **2002**, *6*, 187.
[10] Ullmann's Encyclopedia of Industrial Chemistry, 5th ed., vol. A 19, VCH Weinheim, Germany **1991**, p. 573–597.
[11] D. Wöhrle, M.W. Tausch, W.D. Stohrer, 'Photochemie', Wiley-VCH, Weinheim, Germany **1998**, p. 313–337.
[12] Organikum, 21th ed., Wiley VCH, Weinheim, Germany **2001**, p. 367–372.
[13] Ullmanns Encyklopädie der technischen Chemie, 3th ed., vol. 8, Urban & Schwarzenberg, München, Germany **1957**, p. 429.
[14] R.H. Perry, D.W. Green, 'Perry's Chemical Engineer's Handbook', 7th ed., McGraw-Hill, New York **1997**, p. 6–43.
[15] C. Wille, PhD thesis, Technische Universität Clausthal **2000**.
[16] P. Beltrame, S. Carra, *Tetrahedron Lett.* **1965**, *6*, 3909.